

Contribution from the Evans Chemical Laboratory,
The Ohio State University, Columbus, Ohio 43210

Dinuclear Iron(II) Complexes Showing Unusual Reversible Oxidation-Reduction Behavior with Dioxygen

NORMAN HERRON, WAYNE P. SCHAMMEL, SUSAN C. JACKELS, JOSEPH J. GRZYBOWSKI, L. LAWRENCE ZIMMER, and DARYLE H. BUSCH*

Received April 28, 1982

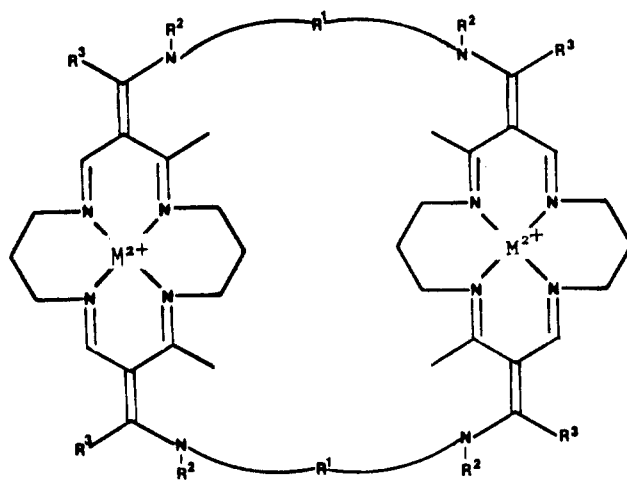
A series of dinuclear iron(II) complexes of novel face-to-face compartmental ligands has been prepared and characterized. The complexes are related to previously reported mononuclear lacunar complexes and possess a large permanent void between the metal ions. Their interactions with axial bases and CO are described. The complexes undergo a net 2-electron oxidation-reduction reaction with dioxygen, generating superoxide or peroxide (depending on solvent) and the complex in which the two irons are identical and are in the low-spin, trivalent state. Remarkably, this net redox reaction can be partially reversed by the removal of O_2 , by N_2 flushing or dynamic vacuum, in mixed aqueous solvents at 0 °C. In this way alone the process resembles reversible dioxygen adduct formation. This behavior is contrasted with true dioxygen adduct formation by a related mononuclear five-coordinate iron(II) complex.

Introduction

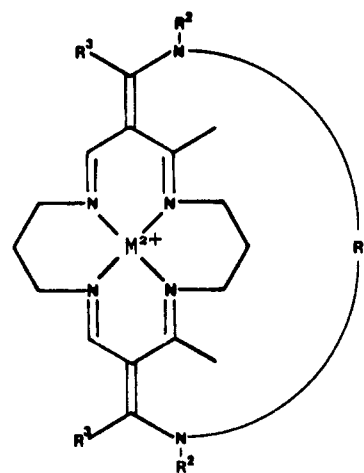
Such natural products as hemerythrin¹ and hemocyanin,² in which reversible dioxygen binding is associated with pairs of metal ions in close proximity, have helped stimulate attention towards binuclear coordination compounds. Synthetic species are typified by so-called *compartmental ligands*, in which coordination sites may occupy side-by-side³ or face-to-face positions.⁴ The face-to-face porphyrins exemplify a second major source of interest in binuclear species, the possibility of facilitating 2-electron or, ideally for O_2 , 4-electron processes.⁵ We wish to report here a new series of dinuclear iron(II) complexes of a face-to-face compartmental ligand (I) that exhibit unusual behavior in their reaction with dioxygen. The compartmental ligands have been previously described as their nickel(II) complexes^{6,7} and represent oligomers of mononuclear species (II) that have been extensively characterized and are called lacunar complexes.⁸ The iron(II) complexes of the lacunar ligands (II) reversibly form dioxygen adducts,⁹ and the dinuclear species reported here also react reversibly with dioxygen but in a totally different manner.

Experimental Section

Physical Measurements. Elemental analyses were performed by Galbraith Labs, Inc., Knoxville, TN. Electronic spectra were recorded on a Cary 17D spectrophotometer in 1-cm gastight quartz cells, fitted with a gas inlet and bubbling tube, from Precision Cells, Inc., Hicksville, NY. Exposure of solutions to a given partial pressure of



I



II

- (1) (a) Stenkamp, R. E.; Jensen, L. H. *Adv. Inorg. Biochem.* **1979**, *1*, 235-252. (b) Loehr, J. E.; Loehr, T. M. *Ibid.* **1979**, *1*, 235-252.
- (2) Schoot Uiterkamp, A. M. J.; Van der Deen, H.; Berendsen, H. C. J.; Boas, J. F. *Biochim. Biophys. Acta* **1974**, *372*, 407.
- (3) (a) Pilkington, N. H.; Robson, R. *Aust. J. Chem.* **1970**, *23*, 2225. (b) Okawa, H.; Tanaka, M.; Kida, S. *Chem. Lett.* **1974**, 987. (c) Fenton, D. E.; Gayda, S. E. *J. Chem. Soc., Dalton Trans.* **1977**, 2109. (d) Glick, M. D.; Lintvedt, R. L.; Anderson, T. J.; Mack, J. L. *Inorg. Chem.* **1976**, *15*, 2258. (e) Gagne, R. R.; Spiro, C. L. *J. Am. Chem. Soc.* **1980**, *102*, 1443.
- (4) (a) Collman, J. P.; Elliott, C. M.; Halbert, T. R.; Tovrog, B. S. *Proc. Natl. Acad. Sci. U.S.A.* **1977**, *74*, 18. (b) Chang, C. K. "Biochemical and Clinical Aspects of Oxygen"; Caughey, W. S., Ed.; Academic Press: New York, 1979; p 437.
- (5) (a) Collman, J. P.; Marrocco, M.; Denisevich, P.; Koval, C.; Anson, F. C. *J. Electroanal. Chem. Interfacial Electrochem.* **1979**, *101*, 117. (b) Collman, J. P.; Denisevich, P.; Kosi, Y.; Marrocco, M.; Koval, C.; Anson, F. C. *J. Am. Chem. Soc.* **1980**, *102*, 6077.
- (6) Busch, D. H.; Christoph, G. G.; Zimmer, L. L.; Jackels, S. C.; Grzybowski, J. J.; Callahan, R. W.; Kojima, M.; Holter, K. A.; Mocak, J.; Herron, N.; Chavan, M.; Schammel, W. P. *J. Am. Chem. Soc.* **1981**, *103*, 5107.
- (7) Busch, D. H.; Jackels, S. C.; Callahan, R. W.; Grzybowski, J. J.; Zimmer, L. L.; Kojima, M.; Olszanski, D. J.; Schammel, W. P.; Stevens, J. C.; Holter, K. A.; Mocak, J. *Inorg. Chem.* **1981**, *20*, 2834.
- (8) Busch, D. H.; Olszanski, D. J.; Stevens, J. C.; Schammel, W. P.; Kojima, M.; Herron, N.; Zimmer, L. L.; Holter, K. A.; Mocak, J. *J. Am. Chem. Soc.* **1981**, *103*, 1472.
- (9) Herron, N.; Busch, D. H. *J. Am. Chem. Soc.* **1981**, *103*, 1236. Herron, N.; Cameron, J. H.; Neer, G. L.; Busch, D. H., submitted for publication.

dioxygen was accomplished by using a series of calibrated rotameters (Matheson, Inc.) to accurately mix oxygen and nitrogen standards and then passing the mixture through the solution in the quartz bubbling cell. Temperature was maintained with use of a Neslab constant-temperature (± 0.3 °C) circulating pump with methanol coolant passing through a Varian variable-temperature cell holder and was measured with a calibrated copper-constantan thermocouple attached to the cell holder itself. IR spectra were recorded on a

Perkin-Elmer 457 or 283B recording spectrophotometer.

Proton NMR spectra were obtained with a Varian Associates 360L spectrometer at 60 MHz while ^{13}C broad-band decoupled NMR spectra were recorded on a Bruker WP-80 spectrometer in the FT mode at 20 MHz. Magnetic susceptibility was measured by using the Evans NMR method¹⁰ on the ^1H , 60-MHz instrument, and Pascal corrections were applied. Deuterated solvents were used throughout, and all chemical shifts are relative to internal Me_4Si on the δ scale ($\delta(\text{TMS}) = 0$). EPR measurements were performed on a Varian E-112 spectrometer in the X band at 9.3 GHz; g values are quoted relative to DPPH ($g = 2.0036$), and samples were either run frozen at -196°C in quartz tubes or run in a Wilmad commercial flat cell as solutions at ambient temperatures.

Electrochemical measurements were made with a Princeton Applied Research Corp. potentiostat-galvanostat, Model 173, equipped with a Model 175 linear programmer and a Model 179 digital coulometer. Current vs. potential curves were measured on a Houston Instruments Model 2000 X-Y recorder. All measurements were performed in a Vacuum Atmospheres glovebox under an atmosphere of dry, oxygen-free nitrogen. The working electrode for voltammetric curves was a platinum disk, with potentials measured vs. a silver wire immersed in 0.1 M silver nitrate in acetonitrile as reference. The working electrode was spun at 600 rpm by a synchronous motor for the rotating platinum electrode (RPE) voltammograms. Peak potentials (E_p) were measured from cyclic voltammograms measured at 50 mV s^{-1} scan rate. Half-wave potentials ($E_{1/2}$) were taken as the potential at half the height of the RPE voltammogram. The value of $|E_{3/4} - E_{1/4}|$ was used as a measure of the reversibility of the couple and was also measured from the RPE voltammogram. All measurements were carried out in solutions containing 0.1 M tetra-*n*-butylammonium tetrafluoroborate as supporting electrolyte.

Kinetic measurements were made with the Cary 17D spectrophotometer and involved exposure of the thermostated solution to a controlled partial pressure of oxygen for 200 s followed by monitoring of spectral absorbance changes (digital readout) as a function of time as measured by a GCA/Precision Scientific timer.

All preparations and manipulations of iron(II) complexes were carried out in a Vacuum Atmospheres glovebox under oxygen-free nitrogen. All chemicals were reagent grade and used without further purification; all solvents were distilled under N_2 before use.

Syntheses. The compartmental ligands were prepared as their pure nickel(II) complexes as previously described.^{6,7} The ligand salts, as HPF_6 derivatives, were also prepared by using methods identical with those already described.^{7,8}

Starting Material for Dinuclear Iron(II) Complexes Where $\text{R}^1 = m\text{-Xylylene}$, $\text{R}^2 = \text{H}$, $\text{R}^3 = \text{CH}_3$. To a suspension of 1.0 g (0.6 mmol) of the $[\text{H}_8((m\text{-xylyl})(\text{NH}_2\text{Et})_2\text{Me}_2[16]\text{tetraeneN}_4)_2](\text{ZnCl}_4)$ ligand salt in 25 mL of acetonitrile were added 0.78 g (1.8 mmol) of tetrakis(pyridine)iron(II) chloride¹¹ and 0.71 g (7.0 mmol) of triethylamine to give a deep red solution. Rapid filtration followed by overnight stirring produced a bright red precipitate. The product was collected, washed with acetonitrile and ether, and vacuum-dried; yield 0.65 g.

[Bis(pyridine)(2,12,14,20,22,32,34,40-octamethyl-3,11,15,19,23,31,35,39,42,46,50,54-dodecaazapentacyclo[31.7.7.^{13,21}.1.^{5,9}.1.^{25,29}]hexapentaconta-1,5,7,9(56),12,14,19,21,25,27,29(48),32,34,39,41,46,49,54-octadecaene- $\kappa^8\text{N}$)diiron(II)] Hexafluorophosphate, [(Fe-py)₂((*m*-xylyl)(NH₂Et)₂Me₂[16]tetraeneN₄)₂](PF₆)₄ ($\text{R}^1 = m\text{-Xylylene}$, $\text{R}^2 = \text{H}$, $\text{R}^3 = \text{CH}_3$, $\text{M} = \text{Fe-py}$). A 1-g quantity of crude starting material from above was dissolved in 100 mL of methanol and filtered. A 3.0-g amount of pyridine (38 mmol) was added and the solution volume reduced to 50 mL. A 2-g quantity of NH_4PF_6 (12.3 mmol) in a minimum volume of methanol was added dropwise to yield a red precipitate. Washing with methanol and then ether and vacuum drying yields 0.9 g (58%) of the product. Anal. Calcd for $[\text{Fe}_2\text{C}_{62}\text{H}_{82}\text{N}_{14}\text{P}_4\text{F}_{24}]$: C, 43.42; H, 4.82; N, 11.43; Fe, 6.51. Found: C, 43.51; H, 4.96; N, 11.33; Fe, 6.23.

[Bis(pyridine)(2,7,9,15,17,22,24,30-octamethyl-3,6,10,14,18,21,25,29,32,36,39,43-dodecaazatetracyclo[21.7.7.^{8,16}]tetratetraconta-1,7,9,14,16,22,24,29,33,38,43-dodecaene- $\kappa^8\text{N}$)diiron(II)] Hexafluorophosphate, [(Fe-py)₂((CH₂)₂(NH₂Et)₂Me₂[16]tetraeneN₄)₂]

(PF₆)₄ ($\text{I: R}^1 = (\text{CH}_2)_2$, $\text{R}^2 = \text{H}$, $\text{R}^3 = \text{CH}_3$, $\text{M} = \text{Fe-py}$). A 500-mg amount (0.2 mmol) of the ligand salt $[\text{H}_8((\text{CH}_2)_2(\text{NH}_2\text{Et})_2\text{Me}_2[16]\text{tetraeneN}_4)_2](\text{PF}_6)_2$ and 170 mg (0.6 mmol) of bis(pyridine)-iron(II) chloride¹¹ were stirred in 25 mL of dry acetonitrile. Addition of 300 mg (2.8 mmol) of triethylamine turned the pale orange solution to a deep clear red. The solution was refluxed for 10 min and filtered through Celite and then left for 1 h before evaporating to dryness. Dissolution in hot methanol and addition of 500 mg of NH_4PF_6 in methanol and 0.5 mL of pyridine precipitated a bright red powder, which was collected, washed extensively with alcohol, and dried; yield 209 mg (65.6%). Anal. Calcd for $[\text{Fe}_2\text{C}_{50}\text{H}_{74}\text{N}_{14}\text{P}_4\text{F}_{24}]$: C, 38.43; H, 4.77; N, 12.55. Found: C, 38.43; H, 4.82; N, 12.60.

[Bis(pyridine)(2,8,10,16,18,24,26,32-octamethyl-3,7,11,15,19,23,27,31,34,38,41,45-dodecaazatetracyclo[23.7.7.^{9,17}]hexatetraconta-1,8,10,15,19,23,27,31,34,38,41,45-dodecaene- $\kappa^8\text{N}$)diiron(II)] Hexafluorophosphate, [(Fe-py)₂((CH₂)₃(NH₂Et)₂Me₂[16]tetraeneN₄)₂](PF₆)₄ ($\text{I: R}^1 = (\text{CH}_2)_3$, $\text{R}^2 = \text{H}$, $\text{R}^3 = \text{CH}_3$, $\text{M} = \text{Fe-py}$), and [Bis(pyridine)(2,9,11,17,19,26,28,34-octamethyl-3,8,12,16,20,25,29,33,36,40,43,47-dodecaazatetracyclo[25.7.7.^{10,18}]octatetraconta-1,9,11,16,18,26,28,33,35,40,42,47-dodecaene- $\kappa^8\text{N}$)diiron(II)] Hexafluorophosphate-2-Methanol, [(Fe-py)₂((CH₂)₄(NH₂Et)₂Me₂[16]tetraeneN₄)₂](PF₆)₄·2MeOH ($\text{I: R}^1 = (\text{CH}_2)_4$, $\text{R}^2 = \text{H}$, $\text{R}^3 = \text{CH}_3$, $\text{M} = \text{Fe-py}$). Both of these dinuclear complexes were prepared by routes identical with those described for $\text{R}^1 = (\text{CH}_2)_2$ above. For $\text{R}^1 = (\text{CH}_2)_3$ the yield was 72%. Anal. Calcd for $[\text{Fe}_2\text{C}_{57}\text{H}_{78}\text{N}_{14}\text{P}_4\text{F}_{24}]$: C, 39.26; H, 4.94; N, 12.33. Found: C, 39.30; H, 5.15; N, 12.41. For $\text{R}^1 = (\text{CH}_2)_4$ the yield was 58%. Anal. Calcd for $[\text{Fe}_2\text{C}_{56}\text{H}_{90}\text{N}_{14}\text{O}_2\text{P}_4\text{F}_{24}]$: C, 39.96; H, 5.39; N, 11.65. Found: C, 39.93; H, 5.23; N, 11.66.

[Bis(pyridine)(2,12,14,20,22,32,34,40-octamethyl-3,11,15,19,23,31,35,39,42,46,49,53-dodecaazadecacyclo[31.7.7.^{13,21}.4.^{7,7}.4.^{27,27}.4.^{55,56}.4.^{57,58}.4.^{67,68}.4.^{69,70}]octaheptaconta-1,12,14,19,21,32,34,39,41,46,48,53,55(56),57(58),59,61,63,65,67(68),69(70),71,73,75,77-tetracosae- $\kappa^8\text{N}$)diiron(II)] Hexafluorophosphate, [(Fe-py)₂((C₇Fl)(NH₂Et)₂Me₂[16]tetraeneN₄)₂](PF₆)₄ ($\text{I: R}^1 = 9,9\text{-Bis}(3\text{-propyl})\text{fluorene}$, $\text{R}^2 = \text{H}$, $\text{R}^3 = \text{CH}_3$, $\text{M} = \text{Fe-py}$). A 1.4-g quantity of the ligand salt $[\text{H}_8((\text{C}_7\text{Fl})(\text{NH}_2\text{Et})_2\text{Me}_2[16]\text{tetraeneN}_4)_2](\text{ZnCl}_4)$ and 0.7 g of $\text{Fe}^{\text{II}}(\text{py})_2\text{Cl}_2$ were stirred in 40 mL of warm acetonitrile. Addition of 0.8 g of triethylamine generated a dark red solution, which was filtered and partially evaporated, yielding a gummy red oil. Addition of acetone, an excess of NH_4PF_6 in ethanol, and 0.5 mL of pyridine caused a deepening in color of the clear red solution. Evaporation of the acetone yielded a red precipitate, which was collected, washed with ethanol, and dried. Anal. Calcd for $[\text{Fe}_2\text{C}_{84}\text{H}_{102}\text{N}_{14}\text{P}_4\text{F}_{24}]$: C, 50.36; H, 5.33; N, 9.78. Found: C, 50.62; H, 5.27; N, 9.96.

Dinuclear species containing axial bases other than pyridine (1-Melm, 2-Melm, Im) may be easily prepared by routes identical with those described, by substituting the desired base for pyridine at the appropriate point. In all cases a stoichiometry of one axial base to one iron center is observed.

Dicarbonylbis(pyridine)(2,8,10,16,18,24,26,43-octamethyl-3,7,11,15,19,23,27,31,34,38,41,45-dodecaazatetracyclo[23.7.7.^{9,17}]hexatetraconta-1,8,10,15,19,23,27,31,34,38,41,45-dodecaene- $\kappa^8\text{N}$)diiron(II)] Hexafluorophosphate-2-Methanol, [(FeCO)₂((CH₂)₃(NH₂Et)₂Me₂[16]tetraeneN₄)₂](PF₆)₄·2MeOH ($\text{I: R}^1 = (\text{CH}_2)_3$, $\text{R}^2 = \text{H}$, $\text{R}^3 = \text{CH}_3$, $\text{M} = \text{py-Fe-CO}$). A 220-mg amount of $[(\text{Fe-py})_2((\text{CH}_2)_3(\text{NH}_2\text{Et})_2\text{Me}_2[16]\text{tetraeneN}_4)_2](\text{PF}_6)_4$ (prepared above) was dissolved in 20 mL of warm methanol in the presence of 220 mg of pyridine. The solution was filtered directly into a 50-mL Schlenk flask, removed from the glovebox, and exposed to carbon monoxide gas (Matheson research grade, 99.99%) by vacuum/CO purge cycles. The solution was returned to the glovebox, excess NH_4PF_6 was added, and the solution was evaporated to dryness. Recrystallization of the solid from acetonitrile/methanol (overnight) yielded the desired product. Anal. Calcd for $[\text{Fe}_2\text{C}_{56}\text{H}_{86}\text{N}_{14}\text{O}_4\text{P}_4\text{F}_{24}]$: C, 39.31; H, 5.07; N, 11.46. Found: C, 39.66; H, 5.03; N, 11.66. Other CO adducts were prepared by identical procedures.

[Bis(pyridine)diaquo(2,12,14,20,22,32,34,40-octamethyl-3,11,15,19,23,31,35,39,42,46,50,54-dodecaazapentacyclo[31.7.7.^{13,21}.1.^{5,9}.1.^{25,29}]hexapentaconta-1,5,7,9(56),12,14,19,21,25,27,29(48),32,34,39,41,46,49,54-octadecaene- $\kappa^8\text{N}$)diiron(III)] Hexafluorophosphate-2-Methanol, [(FeOH₂)₂((*m*-xylyl)(NH₂Et)₂Me₂[16]tetraeneN₄)₂](PF₆)₄·2MeOH ($\text{I: R}^1 = m\text{-Xylylene}$, $\text{R}^2 = \text{H}$, $\text{R}^3 = \text{CH}_3$, $\text{M} = \text{py-Fe-OH}_2$). A 300-mg quantity (0.18 mmol) of $[(\text{Fe-py})_2((m\text{-xylyl})(\text{NH}_2\text{Et})_2\text{Me}_2[16]\text{tetraeneN}_4)_2](\text{PF}_6)_4$ (pre-

(10) Evans, D. F. *J. Chem. Soc.* 1959, 2003.

(11) Long, G. J.; Whitney, D. L.; Kennedy, J. E. *Inorg. Chem.* 1971, 10, 1406.

Table I. Electrochemical Data^c for Dinuclear Iron(II) Complexes of Structure I in Various Solvents

R ¹ (R ² = H, R ³ = CH ₃)	acetonitrile (An)			An + excess py ^a			An + excess 1-MeIm ^a		
	E _{1/2} , V	E _{3/4} - E _{1/4} , V	E _p (ox), V	E _{1/2} , V	E _{3/4} - E _{1/4} , V	E _p (ox), V	E _{1/2} , V	E _{3/4} - E _{1/4} , V	E _p (ox), V
(CH ₂) ₂	<i>b</i>	<i>b</i>	-0.18	<i>b</i>	<i>b</i>	-0.18	<i>b</i>	<i>b</i>	-0.47
	<i>b</i>	<i>b</i>	+0.07	<i>b</i>	<i>b</i>	-0.02	<i>b</i>	<i>b</i>	-0.22
(CH ₂) ₃	-0.12	0.07	-0.08	-0.22	0.07	-0.18	-0.55	0.07	-0.52
(CH ₂) ₄	-0.13	0.09	-0.09	-0.21	0.09	-0.16	-0.54	0.07	-0.50
<i>m</i> -xylylene	-0.08	0.09	-0.04	-0.13	0.09	-0.09	-0.48	0.09	-0.44
C ₇ -fluorene				-0.32	0.10	-0.27			

^a Excess base is the quantity beyond which no more shift in the redox potential was observed upon further addition (~1000 equiv).

^b The RPE trace cannot be analyzed since two redox processes occur in close sequence. ^c All data measured in CH₃CN containing 0.1 M (*n*-Bu)₄NBF₄ and referenced to AgNO₃/Ag 0.1 M in CH₃CN (Pt disk electrode, 0.05 V s⁻¹ scan rate, T = 22 °C).

pared above) was dissolved in 10 mL of acetonitrile containing 1 mL of pyridine. A 5-mL amount of methanol, containing 100 mg (0.18 mmol) of ceric ammonium nitrate, was added, producing an immediate color change from red to deep blue-green. The solution was evaporated to dryness, and the solid was dissolved in the minimum volume of methanol. Filtration, followed by addition of 1.0 g of NH₄PF₆ in methanol, resulted in precipitation of a deep green-blue powder, which was collected and recrystallized from methanol containing a little pyridine; yield 145 mg (39%). Anal. Calcd for [Fe₂C₆₄H₉₄N₁₄O₄P₆F₃₆]: C, 36.52; H, 4.50; N, 9.31; Fe, 5.30. Found: C, 36.27; H, 4.66; N, 9.17; Fe, 5.56. The origin of the water in this sample is unclear but may have resulted from the recrystallization process, which was carried out on the benchtop. An IR spectrum of the complex does indicate the presence of OH groups.

Results and Discussion

Synthesis and Characterization. The syntheses of the dinuclear iron(II) species are described in the Experimental Section and represent simple modifications on our previously reported scheme for the synthesis of the related mononuclear complexes.¹² Of particular interest is the fact that the dinuclear species I are usually isolated as their (PF₆)₄ salts with a single neutral axial base per iron atom. This observation stands in marked contrast to that with the mononuclear lacunar complexes II, which generally exist in solution and crystallize as the high-spin five-coordinate chloro complexes^{9,12} under identical synthetic conditions. This difference in behavior probably stems from the ability of the dinuclear species to become six-coordinate in solution (vide infra) much more readily, resulting in a trans labilization of coordinated chloride and its replacement by neutral ligands. Such behavior has been observed with the mononuclear lacunar species¹² when exposed to carbon monoxide. Otherwise, it is difficult to replace the axial chloride of the lacunar complexes by neutral ligands.

The bright red solid dinuclear iron(II) complexes invariably contain only 1 equiv of base/iron atom; however, in solution (CD₃CN) magnetic susceptibility measurements by the Evans method¹⁰ indicate that the iron has the low-spin configuration ($\mu_{\text{eff}} = 0.6 \mu_B$) (I: R¹ = *m*-xylylene, R² = H, R³ = CH₃). This strongly suggests that each iron(II) center of the dinuclear complex readily becomes six-coordinate in such a coordinating solvent. The ¹³C NMR spectrum (Figure 1) of the complex I (R¹ = *m*-xylylene, R² = H, R³ = CH₃) in CD₃CN is clean and sharp, showing that the ligand structure has remained intact.^{6,7} The resonances of the pyridine axial base are considerably broadened, suggesting that they are in relatively slow exchange with bulk acetonitrile and in competition for a binding site on iron(II). Such slow exchange is to be expected for low-spin iron(II) macrocyclic complexes.¹³

The electrochemistry (Table I) of the dinuclear species in acetonitrile solution is complex with multiple redox waves

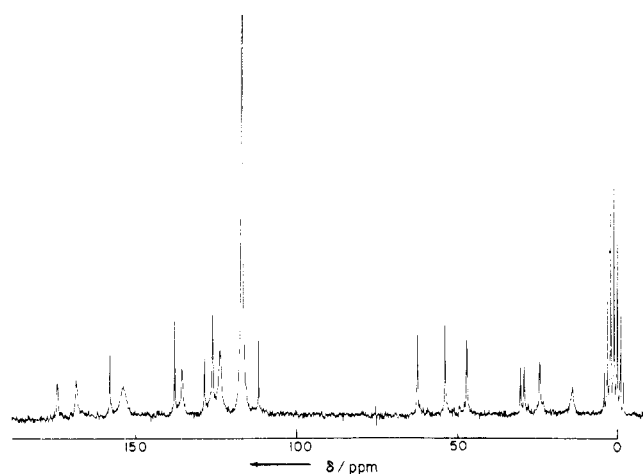


Figure 1. Broad-band decoupled ¹³C NMR spectrum of I, R¹ = *m*-xylylene, R² = H, R³ = CH₃, M = Fe^{II}-py, in CD₃CN at ambient probe temperature (~35 °C).

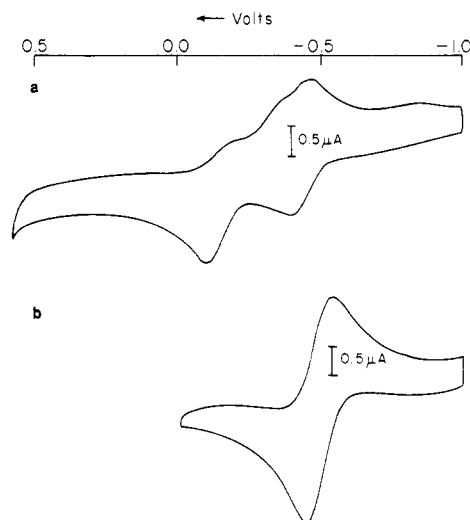


Figure 2. Oxidation processes for I, R¹ = (CH₂)₃, R² = H, R³ = CH₃, M = Fe^{II}-py, by cyclic voltammetry (*n*-Bu₄NBF₄ supporting electrolyte, Ag/AgNO₃ (0.1 M) reference electrode, Pt-disk electrode, 0.05 V s⁻¹ scan rate, T = 22 °C): (a) CH₃CN solution; (b) CH₃CN solution with excess 1-MeIm added (500 equiv).

apparent in the CV voltage region associated with the metal(II/III) couple (Figure 2a). Little consistency between systems is observed and probably reflects the large variety of species possible (i.e., different combinations of base and solvent adducts). In general, the pyridine adducts have E_{1/2} in the region -0.05 to -0.20 V vs. Ag⁰/Ag⁺ in CH₃CN. On addition of excess (~500-fold) axial base to the solutions, however, the electrochemistry improves greatly with the multiple waves collapsing to a single wave (Figure 2b). Addition of excess 1-MeIm generates systems having a more negative potential

(12) Busch, D. H.; Zimmer, L. L.; Grzybowski, J. J.; Olszanski, D. J.; Jackels, S. C.; Callahan, R. W.; Christoph, G. G. *Proc. Natl. Acad. Sci. U.S.A.* **1981**, *78*, 5919.

(13) Holloway, C. E.; Stynes, D. V.; Vuick, C. P. *J. Chem. Soc., Dalton Trans.* **1979**, 124.

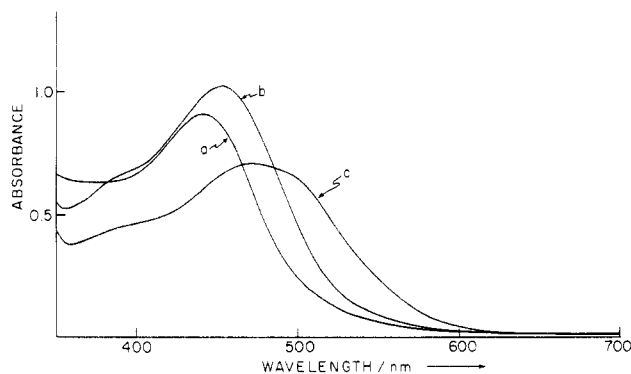


Figure 3. Electronic spectra of I, $R^1 = C_7$ -fluorene, $R^2 = H$, $R^3 = CH_3$, $M = Fe^{II}$ -py, in acetonitrile at 25 °C at a concentration of 4.5×10^{-5} M: (a) no added base ($\epsilon_{441} = 2.02 \times 10^4$); (b) excess pyridine added ($\epsilon_{453} = 2.26 \times 10^4$); (c) excess 1-MeIm added ($\epsilon_{470} = 1.55 \times 10^4$). Extinction coefficients are quoted in $dm^3 \text{ mol}^{-1} \text{ cm}^{-1}$ and relate to two iron chromophore units.

than the corresponding pyridine adducts. No electrochemical evidence for electronic interaction between the metal ions in any complex has been obtained, and this is perhaps not surprising in view of the fact that the corresponding nickel(II) complex also did not display such coupling of redox potentials.^{6,7}

The electronic spectra of the dinuclear complexes (Figure 3) are all extremely similar (for a given axial base and solvent) and, again, strongly support the formulation of the iron(II) centers as being six-coordinate and low-spin in coordinating solvents. The strong charge-transfer band in the 400–500-nm region, which is responsible for the deep red color, is very reminiscent of the $M \rightarrow \pi^*$ transitions of such low-spin tris-(diimine) complexes as $[Fe(o\text{-phen})_3]^{2+}$ or $[Fe(bpy)_3]^{2+}$.¹⁴ In contrast, the five-coordinate lacunar complexes II show only a broad shoulder in the region of 550 nm.⁹

Molar conductances of two of the complexes were measured as 10^{-3} M solutions in acetonitrile. The values 428.4 and 442.4 $\Omega^{-1} \text{ mol}^{-1} \text{ cm}^2$ (for $R^1 = m$ -xylylene, $B = py$ and 1-MeIm, respectively) are in the acceptable range for 4:1 electrolytes in acetonitrile,¹⁵ 370–500 $\Omega^{-1} \text{ mol}^{-1} \text{ cm}^2$.

Axial Ligand Equilibria. As alluded to above, dissolution of any of the pure axial base adducts of the dinuclear complexes in acetonitrile leads to very complex electrochemical behavior that is explicable in terms of multiple axially ligated species in equilibria. A qualitative investigation of these equilibria was carried out for I ($R^1 = m$ -xylylene, $R^2 = H$, $R^3 = CH_3$).

With pyridine as the axial base, in CH_3CN solvent, the electrochemical peak potential E_p of the metal oxidation was found at -0.04 V in the absence of added excess pyridine but shifts to -0.09 V only in the presence of a large excess (Table I). This would suggest that pyridine does not compete with acetonitrile for coordination to iron(II) as strongly as does, say, 1-methylimidazole (see Figure 2). In dimethylformamide solvent the pyridine complex was carefully titrated with excess pyridine. In the absence of excess, the peak potential was -0.355 V vs. Ag/Ag^+ . One equivalent of py shifts the potential to -0.335 V. Further additions result in a limiting E_p of -0.240 V when the $py:Fe(II)$ ratio is $\sim 60:1$. The dinuclear nature of these complexes makes the potential axial equilibria involved very complex, since one or two molecules of axial base or solvent can interact with each metal center. The possibility that, inside the cavity, the axial ligands interact sterically with each other, causing the equilibria at one center to be affected by the coordination status of the other, adds to this complexity.

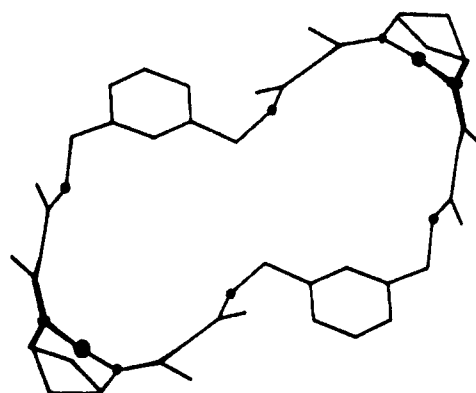
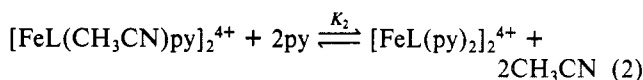
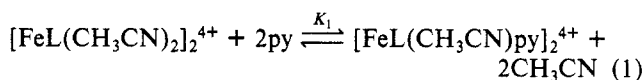


Figure 4. Schematic of the crystal structure of I, $R^1 = m$ -xylylene, $R^2 = H$, $R^3 = CH_3$, $M = Ni^{2+}$ (nitrogens are shaded for clarity).

Electronic spectral investigations of the titration of the pyridine adduct with excess pyridine in acetonitrile result in a regular spectral change. The band maximum shifts from 446 to 460 nm, and the intensity increases as py is added. While regular, the changes are not isosbestic, implying the suspected complexity of equilibria (eq 1 and 2, with the assumption of independent metal centers). The fact that, even in the presence of 900 equiv of py, the spectrum is still changing slightly suggests that, even in the simplest possible model, K_2 has a small value.



In order to assess the role of solvent in these equilibria, the pyridine adduct was allowed to react with excess pyridine in acetone. The observed spectral changes are much larger, and all equilibria appear to be saturated in a 900-fold excess of pyridine. This result verifies the suggestion that pyridine must compete with solvent for an iron(II) binding site since acetone is a weaker axial ligand than acetonitrile. The behavior described above has been observed in all cases and with a variety of axial bases (pyridine, 1-methylimidazole, imidazole).

Interaction with Carbon Monoxide. An X-ray crystal structure determination of the nickel(II) complex of structure I ($R^1 = m$ -xylylene, $R^2 = H$, $R^3 = CH_3$) has shown that the two metal ions are separated (by some 13 Å) by a large void bounded by the ligand framework⁶ (Figure 4). The rigidity of the unsaturated, macrocyclic linking groups leads us to believe that this type of structure is retained in solution to a large extent. While we have shown, above, that solvent or base molecules may enter the internuclear void of the molecule and coordinate axially to iron(II) centers, we are particularly interested in the behavior of these complexes with small gaseous molecules such as CO and O₂.

The dinuclear iron(II) complexes interact with CO at ambient temperature in a 50% H₂O/50% 1-MeIm solvent system, and the reaction is spectrally isosbestic and reversible (Figure 5). Upon exposure to CO the band at 495 nm slowly disappears while a shoulder at 380 nm grows in. Exposure to very high vacuum for extended periods of time causes only slight reversal of these changes, but exposure to sunlight greatly accelerates this process. Thus, it appears that the CO is labilized by UV light and is reminiscent of the iron(II) porphyrin systems.¹⁶ The equilibrium constant for CO adduct formation is very large, the equilibrium being saturated upon

(14) Krumholz, P. *J. Am. Chem. Soc.* **1972**, *94*, 7355.

(15) Geary, W. J. *Coord. Chem. Rev.* **1971**, *7*, 81.

(16) Chang, C. K.; Traylor, T. G. *Biochem. Biophys. Res. Commun.* **1975**, *62*, 729.

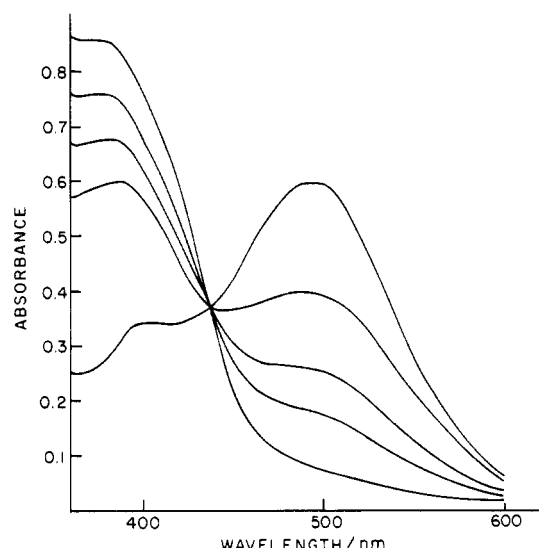


Figure 5. Reversible interaction of increasing partial pressures of CO with I, $R^1 = m$ -xylylene, $R^2 = H$, $R^3 = CH_3$, $M = Fe-1-MeIm$, in 1:1 $H_2O/1-MeIm$ at 0 °C indicated by electronic spectra. Growth of the band at 380 nm accompanies carbonyl adduct formation.

exposure to our lowest accessible partial pressure of CO, i.e., $K_{CO} > 100 \text{ torr}^{-1}$. This is not too surprising since the CO is not expected to be sterically hindered by the ligand as is the case with the mononuclear lacunar complexes.¹² The CO stretching frequencies of the adducts, with pyridine axial base, all center around 1970 cm^{-1} ($R^1 = m$ -xylylene, 1973 cm^{-1} ; $R^3 = C_7\text{fluorene}$, 1973 cm^{-1} ; $R^1 = (CH_2)_3$, 1970 cm^{-1}). It is apparent that ν_{CO} is quite insensitive to the nature of the bridging groups linking the two macrocycles; this is consistent with the idea, expressed above, that the CO is not sterically affected by the ligand framework. It is reassuring to note that these frequencies are very similar to that observed for the unbridged mononuclear carbonyl complex II ($R^1 = CH_3$, $R^2 = CH_3$, $R^3 = CH_3$,¹⁷ $M = Fe-CH_3CN$), 1975 cm^{-1} , which is also expected to have an unencumbered Fe-C-O linkage.

Interaction with O_2 . The possibility of simultaneous binding of one O_2 to the two iron(II) atoms of a single complex of structure I is obviated by the fact that the metal ions are separated by a very large rigid void (e.g., 13.7 \AA as shown by the X-ray crystal structure⁶ of the corresponding Ni^{II} complex for $R^1 = m$ -xylylene, $R^2 = H$, $R^3 = CH_3$ (Figure 4)). The rigidity of the void arises not from the nature of the linking group R^1 but rather from the disposition of the unsaturated chelate rings of the macrocycle portions of the molecule, as illustrated in Figure 4. Chang^{4b} has claimed that metal-metal separations of 5.4 \AA , or greater, favor the binding of two O_2 molecules one to each metal ion in face-to-face porphyrins. None of our complexes have internuclear separations less than 8.5 \AA , based on molecular models. The following discussion is specific for the complex of the crystal structure⁶ shown in Figure 4, but the behavior of the other dinuclear species appears to be identical.

The interaction of the complex with dioxygen presents a most interesting series of chemical changes. Dissolution in a variety of solvents ranging from pure water to pure axial base (1-methylimidazole or pyridine) and mixtures thereof gives a cherry red solution that turns green upon exposure to dioxygen. Curve 1 of Figure 6 shows the original spectrum with a strong absorption band at 498 nm. Curve 2 shows the spectrum after the solution has been saturated with pure O_2 gas at 0 °C; the band at 498 nm has almost disappeared, and a new band has appeared at 750 nm. If the oxygenated so-

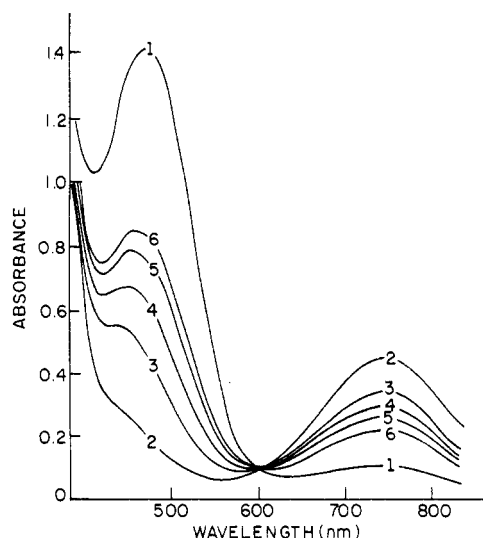


Figure 6. Reversible interaction of O_2 with the binuclear iron(II) complex as indicated by electronic spectra in 1:1 $H_2O/1-MeIm$ at 0 °C: (1) spectrum of original iron(II) complex in solution; (2) spectrum after pure O_2 is bubbled through the solution at 1 atm; (3–6) spectra after successive cycles of flushing with N_2 followed by freezing and evacuating.

lution is subjected to successive freeze-pump-thaw cycles (curves 3–6), the band at 498 nm reappears and continually increases in intensity. The band at 750 nm decreases correspondingly while an excellent isosbestic point persists near 600 nm. Clearly dynamic vacuum produces some reversibility in the reaction with O_2 . Essentially the same results are obtained at room temperature. It is tempting to presume that an iron(II)- O_2 adduct has formed reversibly as has been found for the mononuclear lacunar complexes II;⁹ however, this is not the case.

Simple, straightforward observations are inconsistent with the presence of an O_2 adduct of the usual kind or kinds.¹⁸ The electronic spectrum of the reaction product has maxima at 380 and 750 nm whereas the spectrum of the O_2 adduct of the electronically very similar mononuclear lacunar iron(II) complexes (structure II)⁹ has bands at 521 and 610 nm; clearly, different species are formed in the two cases. Even though the spectral behavior summarized in Figure 6 was consistently isosbestic in numerous experiments, the system invariably reverses only to some 50–70%. These results are not consistent with the usual behavior of reversible O_2 adducts wherein irreversibility always destroys the isosbestic behavior.¹⁹ It is assumed, therefore, that over short time periods (minutes) all of the iron remains in one of the forms involved in the reversible reaction with O_2 but that a second colorless product, formed from the O_2 , is destroyed, thereby limiting the extent of the reverse reaction (O_2^- , H_2O_2 ; vide infra). In support of this suggestion, the addition of a reducing agent (e.g., ascorbic acid) restores the original spectrum almost quantitatively (>90%). Further, the reaction stops completely when the solution is cooled to $-35 \text{ }^\circ\text{C}$; the thermodynamics of O_2 adduct formation require the O_2 affinity to increase as the temperature is lowered.¹⁸ The contrasting behavior we have observed implies the necessity for generation of a coordinatively unsaturated iron(II) complex for reaction to occur (vide infra).

Exposure of a solution of I to 0.2 torr of O_2 for successive time periods, interspersed by brief N_2 purges (Figure 7, curves 1–5), reveals that the reaction with O_2 is slow and that it does not reverse easily. The slow reaction can be driven to com-

(18) Jones, R. D.; Summerville, D. A.; Basolo, F. *Chem. Rev.* **1979**, *79*, 139.

(19) The isosbestic behavior occurs because $\epsilon_A = \epsilon_B$ at λ_{isos} and because $C_A + C_B = \text{constant}$. Either the appearance of a new chromophore (ϵ_C) or the disappearance of some of the iron from $C_A + C_B$ would interfere.

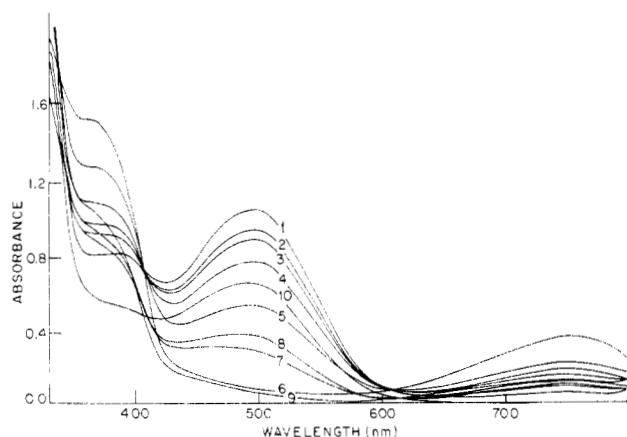
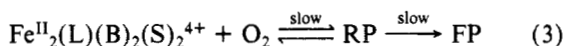


Figure 7. Rate process during O_2 uptake and slow irreversible behavior of the binuclear iron(II) complex as shown by electronic spectra in 1:1 $H_2O/1-MeIm$ at $0^\circ C$ (graphs are numbered in sequence of experiments): (1) spectrum of original iron(II) complex in solution; (2) spectrum after bubbling N_2 containing 0.2 torr of O_2 for 180 s; (3) spectrum after bubbling pure N_2 for 180 s; (4) spectrum after bubbling pure N_2 for 500 s; (5) spectrum after bubbling N_2 containing 0.2 torr of O_2 for 300 s; (6) spectrum after bubbling pure O_2 for 180 s; (7) spectrum after bubbling pure N_2 for 1500 s; (8) spectrum after bubbling pure N_2 for 500 s; (9) spectrum after bubbling pure O_2 for 180 s; (10) spectrum after addition of ascorbic acid to the solution.

pletion by exposure to 760 torr of O_2 for 200 s (Figure 7, graph 6) with only slight deviation from isosbestic behavior. Prolonged flushing with N_2 causes some reversal of the oxygenation reaction, but it is accompanied by complete loss of isosbestic behavior, indicating the onset of a successive reaction (Figure 7, curves 7 and 8).

These observations suggest a model in which the slow production of the reversibly formed products, RP (eq 3), is



followed by the still slower conversion of RP into final products, FP, by an irreversible process. The true nature of the reversible reaction between I and O_2 is elucidated by identification of RP. It is important, in this regard, to know that both iron(II) atoms in solutions of the starting material have the low-spin configuration (see above) and that the 498-nm band is typical of charge-transfer transitions for each species. The nature of FP is most likely a μ -oxo oligomer of the RP formed in the basic medium. Since the EPR spectrum of this oxidized Fe(III) species shows no absorptions for either high- or low-spin iron(III), we are left to postulate an antiferromagnetically coupled iron(III) oligomer of the μ -oxo dimer type.¹⁸

The formation of RP is accompanied by the complete disappearance of the 498-nm band, indicating that both iron(II) atoms have undergone complete reaction. The magnetic moment of the iron complex in RP is $\sim 1.8 \mu_B/\text{iron}$ (Evans method, 5:1:1 $CD_3CN/H_2O/1\text{-methylimidazole}$ at room temperature). These changes are consistent with oxidation of the two low-spin iron(II) centers to two independent low-spin iron(III) centers.

The ESR spectrum of RP (Figure 8) in 1:1 1-MeIm/ H_2O is consistent with the presence of two identical low-spin iron(III) centers, showing the three expected resonances²⁰ at $g = 1.94, 2.14$, and ~ 2.49 . The signal disappears at the rate expected for the conversion of RP into FP. While the ESR results show that there is only one ESR-active species present, they do not rule out the possibility of other oxidized ESR-silent species such as μ -oxo Fe(III) oligomers. Electrochemical

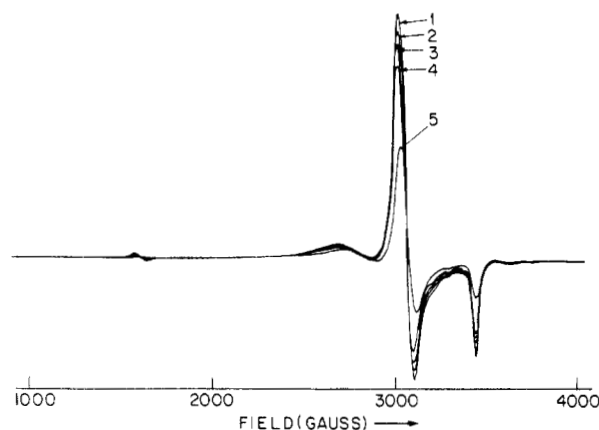
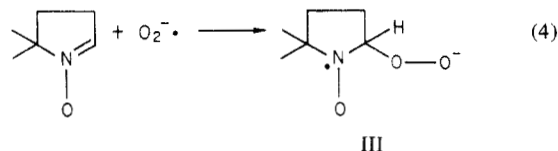


Figure 8. EPR spectra of the reversibly formed, short-term product of the interaction of the binuclear iron(II) complex with dioxygen. The most intense spectrum was measured immediately after exposure to O_2 (60 s). Successive spectra show disappearance of the species with time: (1) 60 s; (2) 1200 s; (3) 3000 s; (4) 5400 s; (5) 8000 s. Spectra were taken at $-196^\circ C$ in 1:1 $H_2O/1-MeIm$. Exposure to O_2 was at $0^\circ C$.

studies show that RP contains a single form of iron(III) and that it is the electrode-couple partner of the iron(II) in the starting complex. There is no evidence for other reducible species (e.g., iron(IV), etc.). In addition, the product (RP) is identical with the independently prepared iron(III) species (Ce^{4+} oxidation) dissolved in the same solvent (same EPR and electronic spectrum) and, furthermore, addition of 1 equiv of H_2O_2 /binuclear iron(III) unit followed by extensive flushing with N_2 results in spectral changes consistent with partial generation of new iron(II) centers. It is clear, therefore, that peroxide and iron(III) are in equilibrium with oxygen and iron(II).

The combined results support the following interpretation. The reversibly formed products (RP in eq 3) in protic media (1:1 base-water) are the low-spin solvated iron(III) complex and peroxide. The question then arises as to whether the iron centers act concertedly to form the peroxide or whether the reaction proceeds via a superoxide intermediate followed by disproportionation to peroxide in these protic media. Strong evidence for the intermediacy of superoxide comes from aprotic EPR experiments using the spin trap 5,5-dimethyl-1-pyrroline 1-oxide.²¹ With use of this reagent in neat anhydrous pyridine solvent, solution EPR spectra, after the iron(II) complex is exposed to dioxygen, clearly show the presence of a trapped superoxide radical (eq 4). The coupling constants of the



resultant nitroxide are identical with those of that produced by adding fresh KO_2 to an anhydrous pyridine solution of the spin trap; $A_H = 13.5 \text{ G}$, $A_N = 11.5 \text{ G}$. Also, since the reversible reaction of I with dioxygen occurs even in anhydrous pyridine as solvent (where generation of free nonprotonated peroxide ion is thermodynamically prohibited), it is clear that a superoxide-mediated mechanism is most attractive. Experiments utilizing the spin trap in partially aqueous media were unable, however, to detect the presence of superoxide. This may well be due to the rapid disproportionation of superoxide or rapid decomposition of the trapped peroxy spin adduct III in these solvents.²²

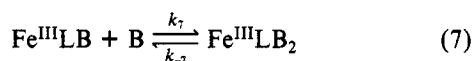
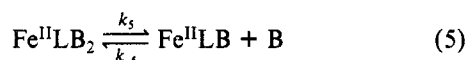
(20) Smith, T. D.; Pilbrow, J. R. *Biol. Magn. Reson.* **1980**, *2*, 85.

(21) Evans, C. A. *Aldrichimica Acta* **1979**, *12* (2), 23. Jantzen, E. G. *Acc. Chem. Res.* **1971**, *4*, 31.

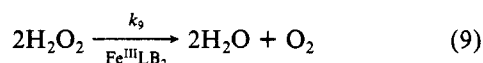
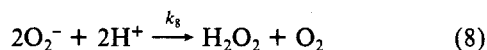
The mononuclear unbridged iron(II) complex of structure II ($R^1 = R^2 = R^3 = \text{CH}_3$,¹⁷ see section on CO binding), which, like the dinuclear species, is low spin and six-coordinate, displays reversible redox behavior almost identical with that of dioxygen in aprotic media (pyridine) and protic media (water/pyridine mixtures). This unbridged complex has an electronic spectrum almost identical with those of the binuclear species ($\lambda_{\text{max}} = 475 \text{ nm}$ in pyridine), which, upon exposure to dioxygen, isospectically (600 nm) changes to the same type of final spectrum. Flushing of this solution with N_2 for extended periods results in partial recovery of the original Fe(II) spectrum to some 30% in 30 min. Re-exposure to O_2 again removes the Fe(II) band at 475 nm exactly as observed for the binuclear complexes. While the overall spectral behavior is the same for both unbridged monomer and binuclear species, the rate and percentage reversibility of the reaction with O_2 are much lower with the monomer. Again, EPR shows that, in neat aprotic pyridine solvent, superoxide ion is generated during the redox process. This evidence again tends to indicate that the two iron centers of the dinuclear species act totally independently of one another with superoxide as the logical reaction intermediate and peroxide as the eventual product of its disproportionation, in protic media.

Mechanism of the O_2 Reactions. The deviation from complete reversibility of the dioxygen reaction results from the known catalase or superoxide dismutase activity of the iron(III) complexes of this class of ligand. The iron complex catalyzes the decomposition of peroxide or superoxide. This permits the reaction with dioxygen to remain isosbestic, despite limited reversibility, because the sum of the concentrations of the two colored iron species always remains constant but the other partner of the reversible reaction, the colorless reduced dioxygen derivative, is partially depleted by the catalase reaction. The occurrence of reversibility is related to the very low (stoichiometric) concentrations of superoxide or peroxide present (which would otherwise reoxidize Fe^{2+}) and the competitive success of the redox process.²³

The combined evidence cited above leads to a probable reaction scheme given by eq 5–10 (with the dinuclear species in both protic and aprotic media



specifically in protic media



treated as two independent iron centers), where L = structure I, $R^1 = m$ -xylylene, $R^2 = \text{H}$, $R^3 = \text{CH}_3$, and B = pyridine solvent and base. This scheme leads to a very complex rate law, which may be considerably simplified if one considers (in

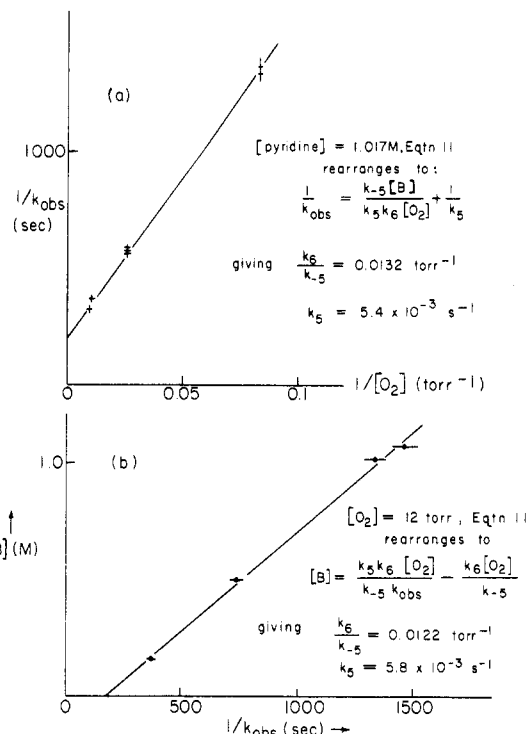


Figure 9. (a) Oxygen and (b) pyridine base dependence of the initial rate of formation of I, $R^1 = m$ -xylylene, $R^2 = \text{H}$, $R^3 = \text{CH}_3$, $M = \text{Fe}^{\text{III}}(\text{py})_2$, from the corresponding Fe^{II} complex (monitored at 520 nm, 0.0 °C, in acetone solvent).

Table II. Rate Data for Reaction of I ($M = \text{Fe}^{\text{II}}$, $R^1 = m$ -Xylylene, $R^2 = \text{H}$, $R^3 = \text{CH}_3$) with Dioxygen in Acetone Solvent at 0.0 °C^c

[B], M	[O ₂], torr	$10^3 k_{\text{obsd}}, \text{s}^{-1}$ ^a	R^b
1.017	12.0	0.75 ± 0.03	0.9928
1.017	38.0	1.7 ± 0.1	0.9934
1.017	38.0	1.79 ± 0.02	0.9986
1.017	38.0	1.74 ± 0.05	0.9951
1.017	99.0	2.68 ± 0.07	0.9941
1.017	105.0	3.06 ± 0.06	0.9955
0.167	12.0	2.8 ± 0.1	0.9965
0.505	12.0	1.36 ± 0.05	0.9939
1.070	12.0	0.68 ± 0.02	0.9997

^a Monitored at 520 nm, absorbance readings taken every 100 s for at least 1500 s. Data were fitted to first-order kinetics with use of the Guggenheim or Keady-Swinbourne method, $\tau = 300 \text{ s}$, to estimate A_∞ . ^b Correlation coefficient R is for the classic first-order linear plot, treated by linear least-squares analysis.

^c Conditions: axial base; B = pyridine; [Fe] in all experiments $1 \times 10^{-4} \text{ M}$.

aprotic media) only the initial rate of the reaction (i.e., ignores k_{-6}) and assumes k_7 is fast (since the six-coordinate Fe^{III} species is the only observed Fe^{III} product). The rate law then simplifies to

$$-\frac{d[\text{Fe}^{\text{II}}\text{LB}_2]}{dt} = \frac{k_5 k_6 [\text{Fe}^{\text{II}}\text{LB}_2][\text{O}_2]}{k_{-5}[\text{B}] + k_6[\text{O}_2]} \quad (11)$$

Iron, oxygen, and base (pyridine) B dependences of the reaction have been investigated and are all in good agreement with this form of the rate law (Table II and Figure 9). The data yield values of $k_5 = (5.6 \pm 0.8) \times 10^{-3} \text{ s}^{-1}$ and the ratio $k_6/k_{-5} = (1.3 \pm 0.4) \times 10^{-2} \text{ torr}^{-1}$ at 0 °C in acetone/pyridine solvent mixtures. The rate of the forward reaction k_5 , loss of the first axial base, is in good agreement with other estimates of the equivalent reaction for other low-spin iron(II) macrocycle complexes.¹³ One important point to be emphasized regarding this kinetic data is the inverse base concentration dependence; i.e., a five-coordinate iron(II) species must be

- (22) Buettner, G. R.; Oberley, L. W. *Biochem. Biophys. Res. Commun.* **1978**, *83*, 69.
 (23) (a) Groves, J. T.; Nemo, T. E.; Myers, R. S. *J. Am. Chem. Soc.* **1979**, *101*, 1032–1033. (b) Chang, C. K.; Kuo, M. S. *Ibid.* **1979**, *101*, 3413–3415. (c) Groves, J. T.; McCluskey, G. A. "Biochemical and Clinical Aspects of Oxygen"; Caughey, W. S., Ed.; Academic Press: New York, 1974; pp 277–309. (d) White, R. E.; Coon, M. J. *Annu. Rev. Biochem.* **1980**, *49*, 315–356.

generated for reaction to occur. This explains why the reaction slows markedly as the temperature is lowered. A point raised by this data is "What is the intimate mechanism of superoxide generation?"; does it, for example, involve formation of a transient oxygen adduct that immediately eliminates superoxide? The reciprocal base dependence of the autoxidation kinetics is most easily interpreted in these terms; however, there are many literature discussions that argue strongly against mechanisms wherein free superoxide is eliminated from an oxygen adduct in aprotic solvents for thermodynamic reasons.²⁴ If this is not the mechanism in our example, how does one then explain the inverse base dependence of the kinetics? One plausible explanation arises from the electrochemical data discussed earlier. We described experiments wherein the addition of increasing amounts of pyridine to one of our iron(II) complexes in DMF leads to a 115 mV positive shift in the metal(II/III) couple. This shift, which makes the metal harder to oxidize, might therefore explain the observed inverse base dependence of the kinetics of autoxidation if the reaction proceeds via our outer-sphere oxidation. As the base concentration increases, the metal gets harder to oxidize and the outer-sphere oxidation reaction slows down. That superoxide ion can be generated in aprotic solvents by outer-sphere oxidation of metal ions by O₂ is well-documented,²⁴ and so this may represent the most realistic intimate mechanism for reaction 6.

Individual components of the overall reaction scheme presented in eq 5-10 have a number of precedents. In particular, reduction reaction 6 is essentially that observed in porphyrin systems when KO₂ reacts with iron(III).²⁵ Reaction

(24) Sawyer, D. T.; Valentine, J. S. *Acc. Chem. Res.* **1981**, *14*, 393-400.

10 is also observed in Fenton type chemistry of iron(III) and peroxide.²⁶ The scheme presented therefore represents a system in which individual, previously noted reactions have combined to produce a deceptively reversible reaction between dioxygen and iron(II) species.

Dioxygen adduct formation by metal atoms in coordination compounds has long been a matter of fundamental interest. Growing activity in application areas assures that their interest will continue. Perhaps the example shown here of a process that superficially appears to involve such an oxygen complex but, in fact, does not will provide some guidance in the clarification of other questionable systems.

Acknowledgment. The financial support of the National Science Foundation is gratefully acknowledged. We wish to thank Madhav Chavan for his assistance in obtaining some of the electrochemical data.

Registry No. I (R¹ = *m*-xylene, R² = H, R³ = CH₃, M = Fe^{II}-py), 85166-57-0; I (R¹ = (CH₂)₂, R² = H, R³ = CH₃, M = Fe^{II}-py), 85166-61-6; I (R¹ = (CH₂)₃, R² = H, R³ = CH₃, M = Fe^{II}-py), 85166-65-0; I (R¹ = (CH₂)₄, R² = H, R³ = CH₃, M = Fe^{II}-py), 85166-67-2; I (R¹ = 9,9-bis(3-propyl)fluorene, R² = H, R³ = CH₃, M = Fe^{II}-py), 85166-69-4; I (R¹ = (CH₂)₃, R² = H, R³ = CH₃, M = py-Fe^{II}-CO), 85166-71-8; I (R¹ = *m*-xylene, R² = H, R³ = CH₃, M = py-Fe^{III}-OH₂), 85185-08-6; [H₈((*m*-xylyl)(NHEthi)₂Me₂[16]-tetraeneN₄)₂](ZrCl₄)₄, 85166-59-2; Fe^{II}(py)₄Cl₂, 15138-92-8; [H₂((CH₂)₂(NHEthi)₂Me₂[16]-tetraeneN₄)₂](PF₆)₂, 85166-63-8; Fe^{II}-(py)₂Cl₂, 15616-26-9; O₂, 7782-44-7; CO, 630-08-0.

(25) McCandlish, E.; Miksztal, A. R.; Nappa, M.; Sprenger, A. Q.; Valentine, J. A.; Strong, J. D.; Spiro, T. G. *J. Am. Chem. Soc.* **1980**, *102*, 4268-4271.

(26) Walling, C.; Partch, R. E.; Weil, T. *Proc. Natl. Acad. Sci. U.S.A.* **1975**, *72*, 140. Walling, C.; Goosen, A. J. *Am. Chem. Soc.* **1973**, *95*, 2987.

Contribution from the Department of Chemistry,
University College, Belfield, Dublin 4, Ireland

Sulfinylaniline Complexes of Iron(0)

HENRY C. ASHTON and A. R. MANNING*

Received August 2, 1982

A number of synthetic routes have been utilized to prepare a series of [Fe(PR₃)₂(CO)₂(ArNSO)] derivatives (I) (R = PhCH₂, 4-MeOC₆H₄, 4-MeC₆H₄, Ph, 4-ClC₆H₄; Ar = 4-MeOC₆H₄, 4-MeC₆H₄, 4-FC₆H₄, Ph, 4-ClC₆H₄, 4-BrC₆H₄, 4-NO₂C₆H₄). The most useful was the reaction of [Fe₂(CO)₉] with PR₃ and ArNSO in tetrahydrofuran at 20 °C, but its efficacy depended on both PR₃ and Ar. In the absence of PR₃, this reaction gave red oils tentatively formulated as [Fe(CO)₄(η¹-(N)-ArNSO)], which with PR₃ rapidly form I. Trialkyl phosphite and alkyl isocyanide nucleophiles displace PPh₃ and/or CO from I with the formation of, e.g., [Fe(PPh₃)(P(OCH₂)₃CMe)(CO)₂(PhNSO)], [Fe(P(OMe)₃)₂(CO)₂(4-NO₂C₆H₄NSO)], or [Fe(PPh₃)₂(CNMe)(CO)(4-NO₂C₆H₄NSO)], but CO displaces the ArNSO ligand. Compounds of type I fail to react with MeI or MeSO₃F, but with other electrophiles such as [4-FC₆H₄N₂]⁺ salts, tetracyanoethylene, or acetic acid, they suffer ArNSO loss with formation of, e.g., [Fe(PPh₃)₂(CO)₂(NNC₆H₄F-4)]BF₄, [Fe(PPh₃)₂(CO)₂-(C₄(CN)₄)] with trans CO ligands, and [Fe(PPh₃)₂(CO)₂(O₂CMe)₂] with cis CO groups. The IR spectra of I have been investigated and absorption bands due to their ν(CO), ν(NS), and ν(SO) vibrations identified and assigned. ArNSO are very powerful electron-withdrawing ligands which thus form stable bonds only with relatively electron-rich metal centers. Metal-to-ligand back-donation appears to be an important, perhaps overwhelming, component of the Fe-ArNSO bond which, it is tentatively concluded, is of the η²-(NS) rather than the η¹-(S) type. The N and S atoms probably lie in the equatorial plane of a trigonally bipyramidally coordinated iron atom while the R₃P ligands occupy the apical coordination positions. The η¹-(S)- and η²-(NS)-ArNSO-metal bonding are outlined in a qualitative fashion, and the reasons for the relative importance of the second as compared with η²-(SO)-SO₂ coordination are discussed.

We have shown previously that the sulfur dioxide complexes [Fe(PR₃)₂(CO)₂(SO₂)] (PR₃ is a phosphine or phosphite ligand) exist in solution as mixtures of the two isomers illustrated in Figure 1.¹ In both there is trigonal-bipyramidal coordi-

nation about the metal atom with the SO₂ ligand in an equatorial position η¹ bonded via S to Fe with the FeSO₂ plane approximately perpendicular to the equatorial plane. In a continuation of this work, we have investigated the preparation, reactions, and IR spectra of the related Fe(0) complexes in which sulfur dioxide has been replaced by sulfinylanilines ArNSO where Ar is a 4-substituted phenyl group.

(1) Conway, P.; Grant, S. M.; Manning, A. R.; Stephens, F. S. *J. Organomet. Chem.* **1980**, *186*, C61.